J. Hydrol. Hydromech., 69, 2021, 1, 1–12
DOI: 10.2478/johh-2020-0038
ISSN 1338-4333

sciendo Journal of Hydrology and Hydromechanics

Spatio-temporal analysis of remotely sensed and hydrological model soil moisture in the small Jičinka River catchment in Czech Republic

Vesna Đukić[1*], Ranka Erić[1], Miroslav Dumbrovsky[2], Veronika Sobotkova[2]

[1] University of Belgrade, Faculty of Forestry, Department of Ecological Engineering for Soil and Water Resources Protection, Kneza Višeslava, 1, 11000 Belgrade, Serbia.
[2] Brno University of Technology, Faculty of Civil Engineering, Institute of Landscape Water Management, Antonínská 548/1, 601 90 Brno, Czech Republic.
[*] Corresponding author. E-mail: vesna.djukic@sfb.bg.ac.rs

Abstract: The knowledge of spatio-temporal dynamics of soil moisture within the catchment is very important for rainfall–runoff modelling in flood forecasting. In this study the comparison between remotely sensed soil moisture and soil moisture estimated from the SHETRAN hydrological model was performed for small and flashy Jičinka River catchment (75.9 km^2) in the Czech Republic. Due to a relatively coarse spatial resolution of satellite data, the satellite soil moisture data were downscaled, by applying the method developed by Qu et al. (2015). The sub-grid variability of soil moisture was estimated on the basis of the mean soil moisture for the grid cell and the known hydraulic soil properties. The SHETRAN model was calibrated and verified to the observed streamflow hydrographs at the catchment outlet. The good correlation between the two different soil moisture information was obtained according to the majority of applied criteria. The results of the evaluation criteria indicate that the downscaled remotely sensed soil moisture data can be used as additional criteria for the calibration and validation of hydrological models for small catchments and can contribute to a better estimation of parameters, to reduce uncertainties of hydrological models and improve runoff simulations.

Keywords: SHETRAN hydrological model; Downscaled remotely sensed soil moisture; Runoff and soil moisture validation; Spatio-temporal variability of soil moisture; Flash floods; Small catchment.

1 INTRODUCTION

The large floods that have occurred in recent years in many regions of the world made local, national and international authorities increasingly aware of flood and inundation hazard and the necessity of a better understanding of floods and flood protection management improvement (IPCC, 2012). Several flash floods occurred in the territory of the Czech Republic during the last decade of June and at the beginning of July 2009, and in May and June 2010 (Danhelka et al., 2014). The hilly and flashy Jičinka River basin (75.9 km^2) in the Moravian - Silesian region in the Czech Republic was particularly affected by serious flooding due to steep slopes of the terrain, and a high percentage of soil types with low-intensity infiltration (Pavlik and Dumbrovský, 2014).

Rainfall–runoff models can be very useful for flash flood forecasting. The runoff generating mechanisms are highly dependant on soil water content. For hydrological modelling and flood forecasting, it is important to understand the spatial-temporal variability of soil moisture at the basin level (Corradini, 2014; Koster et al., 2010; Manfreda et al., 2007; Vereecken et al., 2014). Physically based and distributed models can provide a lot of insight into how soil moisture changes in space and time as a function of terrain, soil and vegetation characteristics of the basin. However, physically based distributed models usually need a large number of parameters (soil surface, soil properties and land use), which can increase the model uncertainty and decrease the performance of the model (Beven, 2006).

The direct ground-based measurements of soil moisture are sufficiently accurate, but are difficult, time-consuming and limited to discrete measurements at particular locations, which makes them unsuitable for hydrological analyses at the basin level (e.g. Brocca et al., 2010; Srivastava et al., 2013; Wang and Qu, 2009).

A useful way to reduce the uncertainty of the model and improve the model performance is to incorporate remotely sensed soil moisture information. Remotely sensed soil moisture provides information about spatial and temporal dynamics of soil moisture, which can facilitate calibration and validation of hydrological models of large scale (see e.g. Albergel et al., 2010; Brocca et al., 2011; Jackson et al., 2010; Parajka et al., 2006; Rötzer et al., 2014). However, due to relatively coarse spatial resolution of approximately several tens of kilometers, satellite soil moisture observations cannot be effectively applied to hydrological studies in small catchments. Due to variations in climate, soil, vegetation, topography and other factors, soil moisture is heterogeneously distributed within catchments.

Over the past decades, various downscaling methods of satellite soil moisture products have been studied for the improvement of their spatial resolution. The variability of soil moisture within a grid cell has often been described by taking into account soil texture (Crow et al., 2012; Gwak and Kim, 2017; Teuling and Troch, 2005), vegetation (Western et al., 1999), topography and other important physical characteristics of the basin which effect the soil moisture (Hupet and Vanclooster, 2002; Koster et al., 2016; Rosenbaum et al., 2012). The estimation of sub- grid variabilty of soil moisture on the basis of soil texture data is facilitated due to the availability of high resolution data on soil properties for the entire globe (Dai et al., 2019; Hengl et al., 2017; Shangguan et al., 2014; Stoorvogel et al., 2017).

A comprehensive review on the downscaling methods for satellite remote sensing based soil moisture is provided in Peng

et al. (2017). They analysed the advantages and limitations associated with each method based on published validation studies. Currently, there are still no effective ways for evaluating either the original remotely sensed soil moisture or the downscaled soil moisture outputs. Usually, the remotely sensed soil moisture products are validated against ground–based soil moisture observations. In general, good agreement was found between downscaled soil moisture and in situ measurements (Lievens et al., 2015; Peng et al., 2017; Verhoest et al., 2015). It was also concluded that the accuracy of the downscaled soil moisture highly depends on the accuracy of the original soil moisture and that it surpasses the original coarse soil moisture for many studies (Peng et al., 2017).

However, the consistency and the level of agreement between downscaled soil moisture and soil moisture simulated by distributed hydrologic models, particualrly in small catchments are still not well understood. The objective of this study is to evaluate the consistency and the agreement between downscaled remotely sensed soil moisture, and soil moisture estimated from the physically based and distributed SHETRAN hydrological model in a small catchment. The evaluation is performed for the small Jičinka River catchment (75.9 km^2) in the Czech Republic during flash floods. The evaluation of modeled soil moisture patterns and their consistency with satellite data during runoff events provides additional information about model reliability and accuracy which is an essential step for the development of soil moisture assimilation strategies in research or operational hydrologic applications.

2 METHOD

2.1 SHETRAN model

SHETRAN is a 3D coupled surface/subsurface physically based and spatially distributed river basin model. SHETRAN (version V4.4.5) water flow component was used in this study. The water flow component consists of 4 modules: evapotranspiration/interception; overland/channel; variably saturated subsurface and snowmelt (Ewen et al., 2000). The components of interception and evapotranspiration were neglected in this study, because their influence is negligible in rain event models. Both the overland and channel flows are described by the diffusive wave approximation of the full St. Venant equations (Saint-Venant, 1871). The continuity equation is as follows:

$$\frac{\partial Q}{\partial x}+\frac{\partial A}{\partial t}=q \tag{1}$$

The momentum conservation is as follows:

$$\frac{\partial Q}{\partial t}+\frac{\partial(\alpha(Q^2/A))}{\partial x}+gA\frac{\partial h}{\partial x}+\frac{gQ|Q|}{C^2AR}=0 \tag{2}$$

where: t is time, x is the distance measured along the channel (m), Q is discharge (m^3 s^{-1}), A is the hydraulic area (m^2), q is the tributary outflow (m^3 s^{-1}), h is the channel depth (m), C is the Chezy coefficient (m$^{0.5}$ s^{-1}), R is the hydraulic radius (m) and α is the correction factor (–).

The soil water movement in the unsaturated zone is described using the Richards equation (Richards, 1931).

The ArcGIS software ArcView 10.2 was used to prepare the input data related to the physical characteristics of the basin and for the displaying and visualisation of the spatially distributed soil moisture values across the basin.

2.2 Calibration and validation of the SHETRAN model

The hydrological model was obtained by the calibration and validation of the SHETRAN model on the basis of the measured streamflow hydrographs at the catchment outlet. The SHETRAN model was calibrated for the storm event which happened in September 2007 and validated for the storm events happened in June 2009, May 2010 and June 2010. In rainfall–runoff modelling, the streamflow is of crucial importance because it reflects the hydrological response of the whole catchment. It was assumed that the good agreement between the modeled and observed runoff hydrographs implies that the other components of hydrological cycle, in this case soil moisture, are appropriately determined.

The area of catchment was discretized into grid cells. The adopted grid cell size in this study is 500 m × 500 m. Although it can be expected that by adopting a coarser grid resolution a lot of spatially important data may have been lost, the use of a coarser grid resolution can be justified when simulating events of high intensity and/or hydrographs with a short concentration time (Molnar and Julien, 2000), as it is the case in the analysed Jičinka River catchment. In the study of Molnar and Julien (2000), it was concluded that a coarser grid resolution can be used in hydrological models as long as parameters are appropriately calibrated.

Through numerous simulations it was concluded that the Strickler's coefficients for overland flow and for river flow, the vertical saturated hydraulic conductivity of the subsurface soil and the saturated water content had an important effect on the size of overland flow. It was also concluded that the values of base flow were dependant on the horizontal saturated hydraulic conductivity in the saturated zone (Đukić and Radić, 2014; Đukić and Radić, 2016). The preliminary values of model parameters used in model calibration were determined from the literature (Table 3) and are presented in the Table 1. The values of all other model parameters were fixed and adopted their average values from the literature (Table 3 and Table 1). The adopted values of all parameters are presented in Table 1.

The agreement between the modelled and observed runoff was evaluated using following objective functions. The first objective function is based on the formulation proposed by Nash and Sutcliffe (1970) and is given by:

$$\mathrm{CR1}=1-\frac{\sum_{i=1}^{n}(Q_{obs,i}-Q_{sim,i})^2}{\sum_{i=1}^{n}(Q_{obs,i}-\overline{Q_{obs}})^2} \tag{3}$$

where: $Q_{obs,i}$ is the observed streamflow on day i, $Q_{sim,i}$ is the simulated streamflow, $\overline{Q_{obs}}$ is the average of the observed streamflow over the calibration (or verification) periods of n days.

Due to changeable variance of model errors, the Nash – Sutcliffe coefficient of efficiency tends to emphasize the large errors. For comparison, the function of Chiew and McMahon (1994) was used as the second objective function in which the square root of the considered values were related using the following equation:

$$\mathrm{CR2}=1-\frac{\sum_{i=1}^{n}\left(\sqrt{Q_{obs,i}}-\sqrt{Q_{sim,i}}\right)^2}{\sum_{i=1}^{n}\left(\sqrt{Q_{obs,i}}-\overline{\sqrt{Q_{obs}}}\right)^2} \tag{4}$$

Table 1. The ranges of model parameters used in calibration of the SHETRAN model, its optimal values (in parenthesis) and the adopted values of uncalibrated parameters for the Jičinka River basin uncalibrated parameters for the Jičinka River basin.

Soil Type	Soil/rock parameters								Land use/ vegetation	Overland flow/channel parameters	
	depth (m)	Texture	k_{vs} (m day^{-1})	k_{hs} (m day^{-1})	θs (–)	θr (–)	α (–)	n (–)		S_t (m$^{1/3}$ s^{-1})	S_{tR} (m$^{1/3}$ s^{-1})
Dystric Cambisol	0–0.7	Sandy clay loam	0.223–0.5814 (0.300)	0.223–0.5814 (0.300)	0.419–0.695 (0.480)	0.047	0.014	1.317	Forest	4–8 (7)	15–40 (30)
	0.7–1.2	Sandy clay loam	0.223–0.5814 (0.300)	0.223–0.5814 (0.300)	0.419–0.695 (0.480)	0.047	0.014	1.317	Arable land	8–20 (18)	
Geological substrate	1.2–4	(sandstone, schists)	4	0.01–5 (4)	0.6	0.1	0.001	1.1	Natural grasslands	7–18 (16)	
Rendzina	0–0.5	Clay loam	0.217–0.4105 (0.270)	0.217–0.4105 (0.270)	0.437–0.442 (0.440)	0.075	0.013	1.415	Scarce vegetation	30–50 (42)	
Geological substrate	1.2–4	(sandstone, schists)	4	0.01–5 (4)							
Eutric cambisol	0–0.5	Clay loam	0.217–0.4105 (0.270)	0.217–0.4105 (0.270)	0.426–0.469 (0.44)	0.075	0.013	1.415			
	0.5–1.05	Loam	0.128–0.192 (0.15)	0.15	0.426–0.469 (0.430)	0.078	0.036	1.56			
Geological substrate	1.2–4	(sandstone, schists)	4	0.01–5 (4)							
Fluvisol	0–0.40	Clay loam	0.217–0.4105 (0.255)	0.217–0.4105 (0.255)	0.426–0.469 (0.430)	0.075	0.013	1.415			
	0.40–1.0	Silty loam	0.130–0.196 (0.163)	0.163	0.452	0.093	0.005	1.68			
	1.0–1.25	Sandy clay loam	0.223–0.5814 (0.300)	0.223–0.5814 (0.300)	0.419–0.695 (0.480)	0.047	0.014	1.317			
Geologic substrate	1.25-4	(sandstone, schists)	4	0.01–5 (4)	0.6	0.1	0.001	1.1			

The third introduced criterion is potentially useful in the context of prediction, for example, where simulations must be as close as possible to the observed values at each time step (Ye et al., 1997). It is defined by:

$$\mathrm{CR3} = 1 - \frac{\sum_{i=1}^{n} \left| Q_{obs,i} - Q_{sim,i} \right|}{\sum_{i=1}^{n} \left| Q_{obs,i} - \overline{Q_{obs}} \right|} \tag{5}$$

The fourth criterion (Pereira and Pruitt, 2004) quantifies the ability of the model to accurately reproduce streamflow volumes over the periods of observation. Criterion CR4 differs from the other three criteria (CR1–CR3), because it does not measure deviation from the observed values at each step of simulation. Therefore, CR4 cannot be used alone as a criterion for calibration. This criterion is defined by:

$$\mathrm{CR4} = \left[1 - \left| \sqrt{\frac{\sum_{i=1}^{n} Q_{sim,i}}{\sum_{i=1}^{n} Q_{obs,i}}} - \sqrt{\frac{\sum_{i=1}^{n} Q_{obs,i}}{\sum_{i=1}^{n} Q_{sim,i}}} \right| \right] \tag{6}$$

In addition to the already mentioned four criteria (CR1–CR4) the following statistical measures were also used: the root-mean-square error (RMSE), the mean absolute error (MAE), the coefficient of correlation (R) and the index of agreement (d). They are expressed by the following equations:

$$MAE = \frac{1}{n} \sum_{i=1}^{n} \left| Q_{obs,i} - Q_{sim,i} \right| \tag{7}$$

$$RMSE = \sqrt{\frac{\sum_{i=1}^{n} (Q_{obs,i} - Q_{sim,i})^2}{n}} \tag{8}$$

$$\mathrm{R} = \frac{\sum_{i=1}^{n} (Q_{obs,i} - \overline{Q_{obs}})\,(Q_{sim,i} - \overline{Q_{sim}})}{\sqrt{\sum_{i=1}^{n} (Q_{obs,i} - \overline{Q_{obs}})^2} \sqrt{\sum_{i=1}^{n} (Q_{sim,i} - \overline{Q_{sim}})^2}} \tag{9}$$

$$d = 1 - \frac{\sum_{i=1}^{n} (Q_{obs} - Q_{sim})^2}{\sum_{i=1}^{n} \left(\left| Q_{sim} - \overline{Q_{obs}} \right| + \left| Q_{obs} - \overline{Q_{obs}} \right| \right)^2}, \quad 0 \le d \le 1 \tag{10}$$

2.2 Downscaling approach for sub-grid variability estimation

The satellite soil moisture data were downscaled by applying the method developed by Qu et al. (2015) in this study. The downscaling approach (Qu et al., 2015) applied in this study is based on the Mualem-van Genuchten (MvG) model, in which the unsaturated soil hydraulic properties are described using the model of van Genuchten (1980) for the water retention function in combination with the hydraulic conductivity function introduced by Mualem (1976). The soil water retention equation, $\theta(h)$, is given by:

$$\theta(h) = \theta_r + \frac{S_e (\theta_s - \theta_r)}{\left[1 + |\alpha h|^n \right]^m} \quad h \le 0 \tag{11}$$

where θ is the volumetric water content (cm^3 cm^{-3}) at pressure head h (cm); θ_s and θ_r are the residual and saturated water content (cm^3 cm^{-3}), respectively; α (cm^{-1}), n (–), and m (–) (m = 1 – 1/n) are shape parameters. The hydraulic conductivity function, $K(h)$, is given by:

$$K(S_e) = K_s S_e^L \left[1 - (1 - S_e^{1/m})^m \right]^2, \quad h \le 0 \tag{12}$$

where K_s is the saturated hydraulic conductivity (cm d^{-1}) and K

(cm d^{-1}) is the hydraulic conductivity and L is the pore connectivity parameter ($L = 0.5$); S_e is effective saturation given by:

$$S_e = \frac{\theta(h) - \theta_r}{\theta_s - \theta_r} \tag{13}$$

For each grid of coarse scale satellite data product, the correlation between the standard deviation and soil moisture $\sigma_\theta(\bar{\theta})$ is expressed as a function of the mean and the standard deviation of the soil hydraulic parameters (K_s, θ_s, θ_r, α, n,) (Montzka et al., 2018) using the following equation:

$$\sigma_\theta^2 = b_0^2 \left\{ \begin{array}{l} b_1^2\sigma_\alpha^2 + b_2^2\left[\frac{\sigma_f^2\rho_f}{(1+a_2\rho_f)a_2} + \frac{a_1\sigma_\alpha^2\rho_\alpha}{(1+a_2\rho_\alpha)a_2} + \frac{a_3\sigma_n^2\rho_n}{(1+a_2\rho_n)a_2}\right] \\ +b_3^2\sigma_n^2 + b_4^2\sigma_{\theta_s}^2 + 2b_1b_2\left(-\frac{a_1\sigma_\alpha^2\rho_\alpha}{1+a_2\rho_\alpha}\right) + 2b_2b_3\left(-\frac{a_3\sigma_n^2\rho_n}{1+a_2\rho_n}\right) \end{array} \right\} \tag{14}$$

f is the log-transformed saturated hydraulic conductivity (ln K_s); ρ is the vertical correlation length of the respective parameters. The coefficients a_1–a_3 and b_0–b_4 are related to the mean of the soil hydraulic parameters: θ_s, θ_r, h, α and n. They are calculated using the equations which are described in papers (Montzka et al., 2018; Qu et al., 2015).

The sub-grid surface soil moisture values can be estimated based on the known average value of surface soil moisture within a grid cell and using the estimated value of the $\sigma_\theta(\bar{\theta})$ function and proxy information. It is supposed that the spatial variability of soil moisture within each coarse scale satellite pixel is related to the known spatial variability of the proxy data (Montzka et al., 2018). By multiplication with the provided soil moisture standard deviation at the given mean surface soil moisture, the sub-grid surface soil moisture values can be calculated using the following equation:

$$\hat{\theta}_{i,j} = \bar{\theta} + \sigma_\theta(\bar{\theta})\frac{P_{i,j} - \bar{P}}{\sigma_p} \tag{15}$$

where: $\hat{\theta}_{i,j}$ is the predicted soil moisture at this fine scale location; $P_{i,j}$ is the proxy data at the fine scale sub-grid y-location i and x-location j, $\bar{P}$ is the mean of the proxy, and σ_P is the standard deviation of the proxy. In this paper the surface soil moisture data were downscaled from its original resolution of 25 km to 1 km resolution. This was done by using the saturated hydraulic conductivity as a proxy for soil moisture heterogeneity. After that, the obtained values of soil moisture were resampled at a 500 m resolution.

2.4 Comparison of surface soil moisture estimates

After the calibration and validation of the SHETRAN model, simulations of soil moisture in unsaturated zone were performed using the sets of parameters optimized for the calibration and the validation rain events. In that way, soil moisture estimates are one of the results obtained by applying the SHETRAN hydrological model.

The consistency between the surface soil moisture simulated by the hydrologic model (SM_{HM}) and the surface soil moisture downscaled from the satellite retrieved soil moisture product (SM_{scatt}) was spatially analyzed using the same criteria which were used for the evaluation of the hydrologic model performance. However, in this case, instead of the simulated (Q_{sim}) and the observed streamflow values (Q_{obs}), the values of SM_{HM} and SM_{scatt} are used in Equations (3) – (10).

3 DATA

3.1 Study area

The Jičinka River basin up to the "Novy Jičin" water level monitoring station (Fig. 1) is situated in the Moravian – Silesian Region, in the eastern part of the Czech Republic. The Jičinka River is a tributary of the Moravice River, which belongs to the basin of the Opava River and to the basin of the Baltic Sea. Altitudes in the Jičinka River basin vary from 270 meters above sea level in the lower part of the basin to 1000 meters in the source areas of the basin. The steep slopes of the terrain in the Jičinka River basin with the average slope of 9.1% significantly affect the characteristics of runoff.

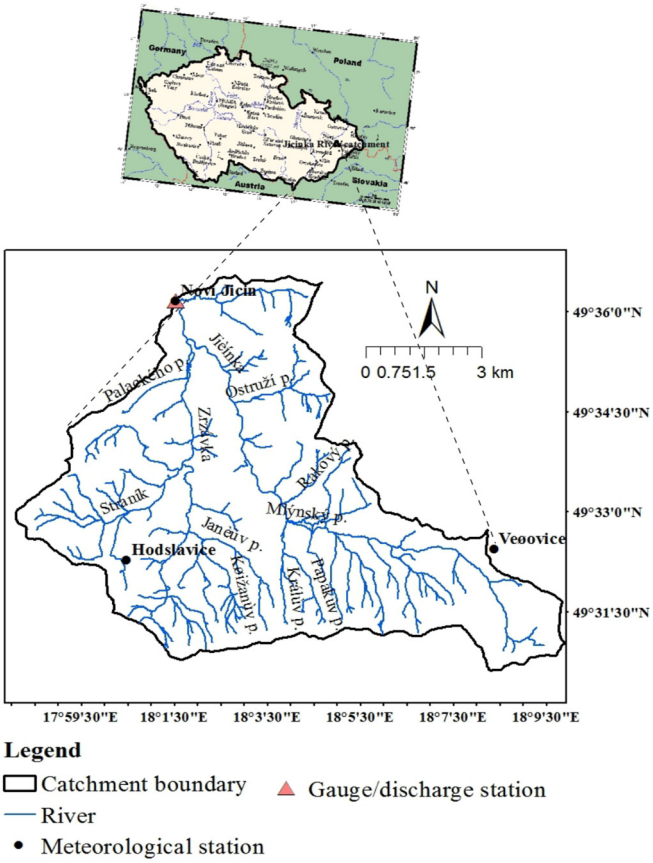

Fig. 1. The Jičinka River basin with the river system and the rain gauging and hydrological stations in the basin.

Four pedological soil types identified in the studied basin include the following: fluvisol (10.5%), eutric cambisol (46.2%), dystric cambisol (41.3%) and rendzina (2%) (Fig. 2). The hydrogeological behaviour of the whole basin is defined by the dominant presence of tertiary and quaternary rocks (sandstones, schists, loess, sand and gravel) which occupy about 75% of the basin (Fig. 2). Four different vegetation types identified in the Jičinka River basin are forest (34%), natural grasslands (48%), arable land (8.5%) and orchards (0.03%) (Fig. 2). Urban areas occupy about 9.4% of the basin area.

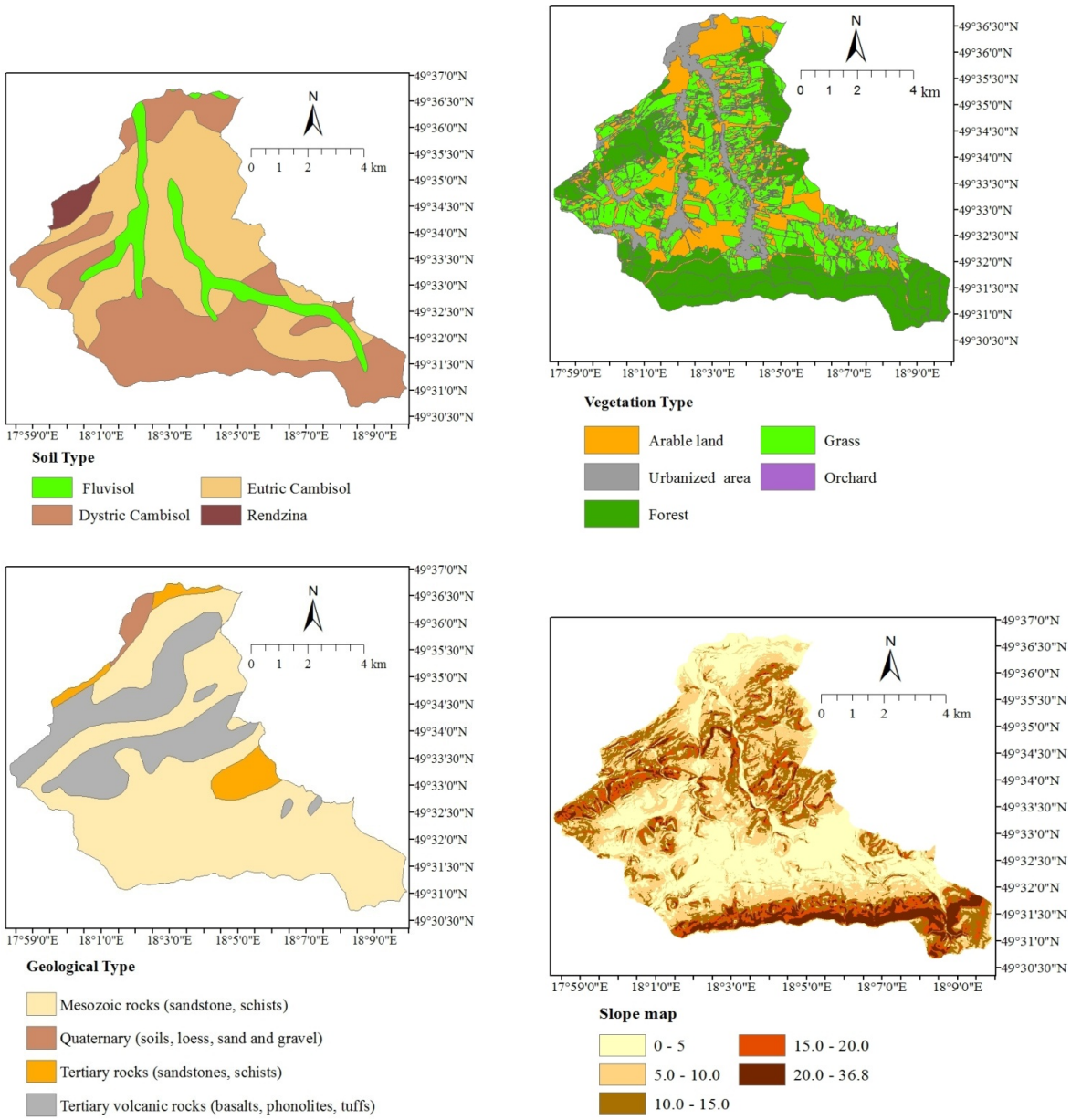

Fig. 2. The map of soil types, vegetation types, geological types and the slope map of the Jičinka River basin up to the "Novy Jičin" water level monitoring station.

Table 2. The total amounts of precipitation (P_{tot}) fallen on the ground, the volume of precipitation (V_p), the maximum runoff value (Q_{max}) and the runoff volume (V_r).

Number of rain event	Simulation period	P_{tot} (mm)	V_p (10^3 m^3)	Q_{max} (m^3/s)	V_r (10^3 m^3)
1	5.09.2007. (10:00) 17.09.2007. (10:00)	190.13	14429.9	98	6387.5
2	22.06.2009. (05:00 – 29.06.2009. (7:00)	150.2	11403	264	5805.5
3	11.05.2010. (13:00 – 29.05.2010. (3:00)	232.8	17670.4	75.6	15666.4
4	30.05.2010. (11:00 – 2.06.2010. (14:00)	46.2	3502.2	43.1	4429.9

3.2 Input data for the SHETRAN model

The average hourly heights of rainfall in the basin during the analyzed rain events were calculated by applying the method of Thiessen polygons (Thiessen, 1911) based on the hourly precipitation levels measured at the climatological stations in the basin (Hodslavice, Verovice and Novy Jičin) (Fig. 1). The hourly values of runoff are measured at the ″Novy Jičin″ hydrological station. The characteristics of precipitation and runoff are presented in Table 2.

The soil, geological, vegetation and slope maps of the Jičinka basin were obtained in the form of vector polygon data at the corresponding digitized maps (Fig. 2). All input data and the corresponding input parameters used in SHETRAN are summarized in Table 3.

Table 3. Input data and parameters used in the SHETRAN model.

Type of input data	Input parameters	Source of input data
Meteorological	Hourly precipitation	Czech Hydrometeorological Institute
Hydrological	Registered streamflow hydrographs	
Topographic	Digital elevation model (DEM) of the resolution: 10 m × 10 m	T.G. Masaryk Water Research Institute
Land use/ vegetation distribution	Strickler's coefficient for overland flow (S_t) and for channel flow (S_{tR}) (Engman,1986)	Corine Land Cover Databases https://land.copernicus.eu/pan-european/corine-land-cover
Soil types	Hydraulic soil/rock properties (porosity and specific storage, residual water content (θ_r), saturated water content (θ_s), vertical saturated hydraulic conductivity (k_{vs}), horizontal saturated conductivity (k_{hs}), van Genuchten - α, van Genuchten - n	http://globalchange.bnu.edu.cn/research/soil5.jsp.
Geological type		″Czech Geological Survey″-ArcGIS online

3.3 Satellite soil moisture data

The satellite soil moisture data used in this study were taken from the European Space Agency (ESA) Climate Change Initiative (CCI) Soil Moisture (SM) project (http://www.esasoilmoisture-cci.org). The ESA CCI SM v04.7 product consists of three surface soil moisture data sets: the "ACTIVE Product", the "PASSIVE Product" and the "COMBINED Product" (Dorigo et al., 2017). The ESA CCI SM product was obtained by combining the soil moisture retrievals from seven passive (SMMR, SSM/I, TMI, AMSR-E, WindSat, AMSR2 and SMOS) and two active (ERS AMI and ASCAT) microwave sensors into a global data set spanning the period 1979 – 2010. The homogenized and merged products present surface soil moisture with a global coverage and a coarse spatial resolution of approximately 25 km and a high temporal resolution of 1 day (Gruber et al., 2019).

In this study the ACTIVE product was used. The "ACTIVE Product" was created by the University of Vienna (TU Wien) based on observations from C-band scatterometers. The sensors ERS AMI and ASCAT operate at similar frequencies (5.3 GHz C-band) and share a similar design. Different algorithms are used for the retrieval of soil moisture from satellite measurements (Gruber et al., 2017).

The ACTIVE soil moisture data are provided in terms of saturation degree [%], ranging between 0 (dry) and 100 (saturated). In this study soil moisture values were used in volumetric units (m^3/m^3). Soil moisture values in volumetric units were calculated by multiplying the degree of saturation by soil porosity (expressed in m^3/m^3). Soil porosity data used in the conversion to volumetric soil moisture measurements have been taken from the GLDAS-Noah dataset (Rodell et al., 2004).

3.4 Soil hydraulic data

The soil hydraulic properties are described using the following parameters: the saturated water content (θ_s), the residual residual water content (θ_r), the saturated hydraulic conductivity (K_s), and the empirical parameters - vanGenuchten - α and van Genuchten - n. These parameters are used in the SHETRAN hydrological model, and they are also used in the applied procedure of soil moisture downscaling from satellite data.

The high resolution soil hydraulic data were taken from the Global Soil Dataset for use in Earth System Models (GSDE) (Shangguan et al., 2014) located at http://globalchange.bnu.edu.cn/research/soil5.jsp. This database provides the global values of soil hydraulic and thermal parameters at the spatial resolution of 30" and for vertical resolutions of: 0 – 0.05 m, 0.05 – 0.15 m, 0.15 – 0.30 m, 0.30 – 0.60 m, 0.60 – 1.00 m, and 1.00 – 2.00 m. Grid maps of hydraulic soil parameters for the Jičinka River catchment, which were derived from the GSDE database, are presented in Fig 3.

4 RESULTS AND DISCUSSION

4.1 Results of the hydrologic model performance evaluation

The comparative overview of the results of the calibration and validation of the SHETRAN model are presented in Fig. 4. The figure shows a close relationship between the modeled and the observed runoff hydrographs. The results of the assessment of the quality of model simulations by applying CR1 – CR4 criteria in Eqs. (3) – (6), and by applying the statistical measures in Eqs. (7) – (9) are presented in Table 4.

On the basis of Table 4, it can be concluded that the good agreement was found between the observed and the modeled streamflow hydrographs for both the calibration and the validation rain events. It should be noted that the best performance measures were observed for the calibration rain event in September 2007 according to the majority of the applied criteria. A small drop in the determined values of the applied criteria from calibration to verification indicates that the model performance decreases only slightly. It should also be noted that there was an improvement of the model performance for the verification rain event in June in 2010 compared to the calibration rain event in September 2007, according to the CR4 criteria, and according to the obtained values of the Mean Absolute Error (MAE) and the Root Mean Square Error (RMSE).

4.2 Comparison of soil moisture estimates

For each of the analyzed rain events grid maps of daily values of soil moisture at a 500 m resolution were created for the two different soil moisture sources. The spatial patterns of the maximum surface soil moisture estimated for the days of the peak runoff occurring during the analysed rain events are presented in Fig. 5.

On the basis of Fig 5. it can be seen that there is an agreement between the soil moisture values simulated by application the SHETRAN model and the values estimated by downscaling from the scatterometer soil moisture data. As it can be expected, the estimated spatially distributed values of soil moisture for the days of the peak runoff occurring during the analysed rain events correspond to the values of the saturated water content in majority of cases for the analysed rain events. Only in the case of the rain event in June 2010, the average daily values of estimated soil moisture are lower in regard to the values of the saturated water content.

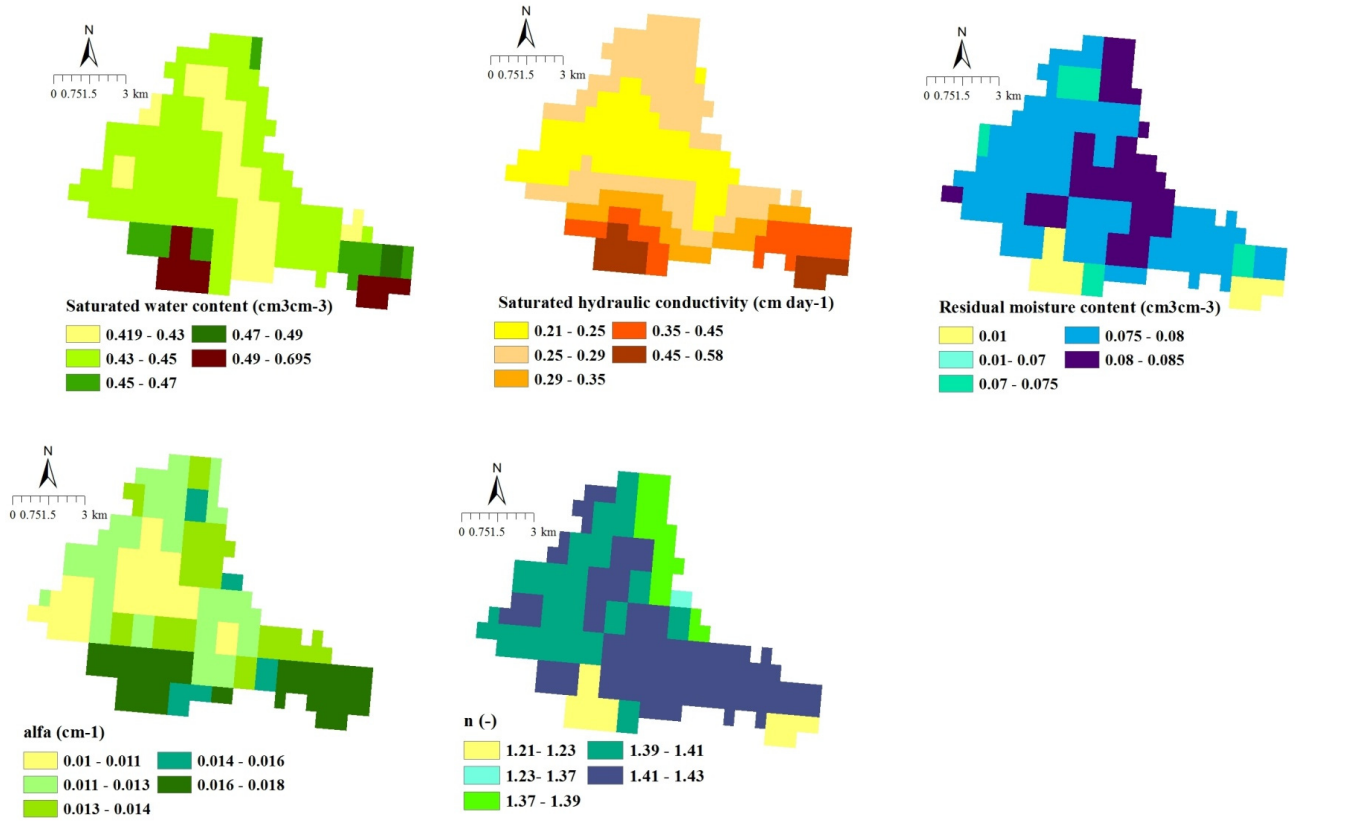

Fig. 3. Grid maps of hydraulic soil parameters for the Jičinka River catchment derived from the GSDE database: saturated water content ($cm^3\ cm^{-3}$), saturated hydraulic conductivity ($cm\ day^{-1}$) residual water content ($cm^3\ cm^{-3}$), and empirical parameters α (cm^{-1}) and n (–).

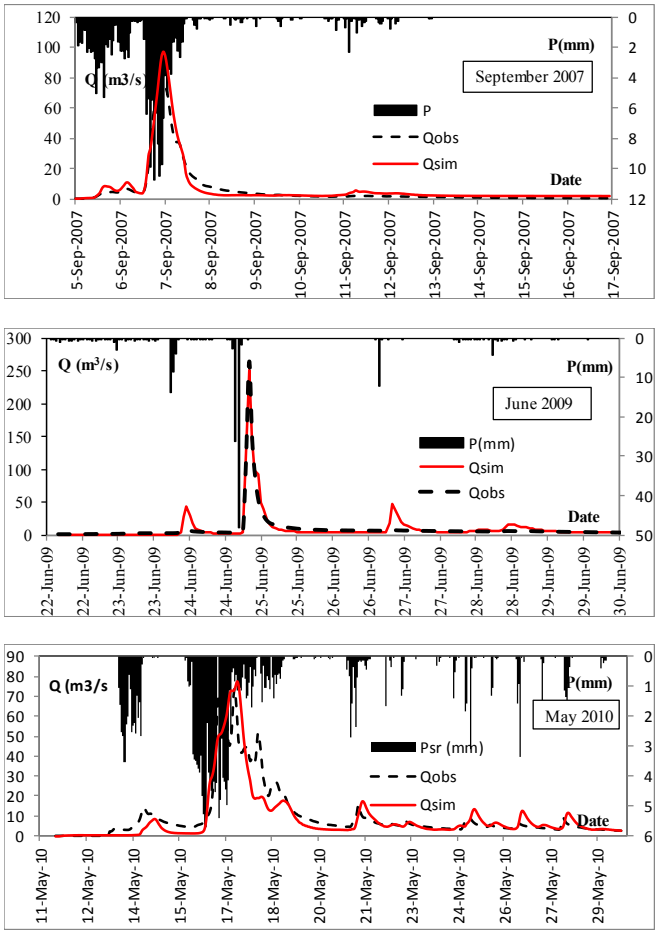

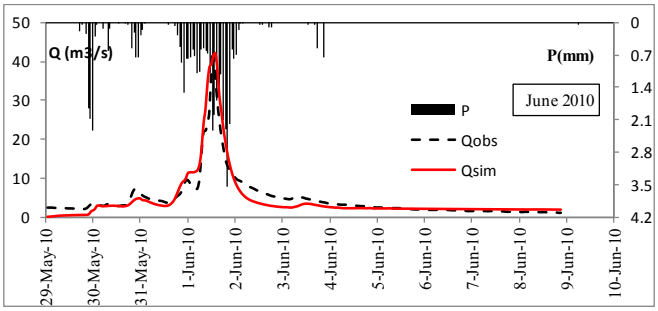

Fig. 4. Observed (Q_{obs}) and the SHETRAN model simulated (Q_{mod}) streamflow hydrographs at the Jičinka River monitoring station (″Novy Jičin″ water level monitoring station) for the calibration (September 2007) and validation (June 2009, May 2010 and June 2010) rain events.

Table 4. The results of the application of criteria CR1–CR4 and statistical measures (MAE, RMSE, R and d) for the assessment of the SHETRAN model simulations.

Criterion	Calibration rain event	Validation rain events		
	September 2007	June 2009	May 2010	June 2010
CR1	0.940	0.905	0.810	0.872
CR2	0.895	0.747	0.803	0.759
CR3	0.720	0.533	0.602	0.577
CR4	0.897	0.786	0.908	0.926
MAE	2.082	3.550	3.412	1.348
RMSE	3.598	7.381	6.036	2.0349
R	0.975	0.961	0.908	0.965
d	0.986	0.978	0.951	0.973

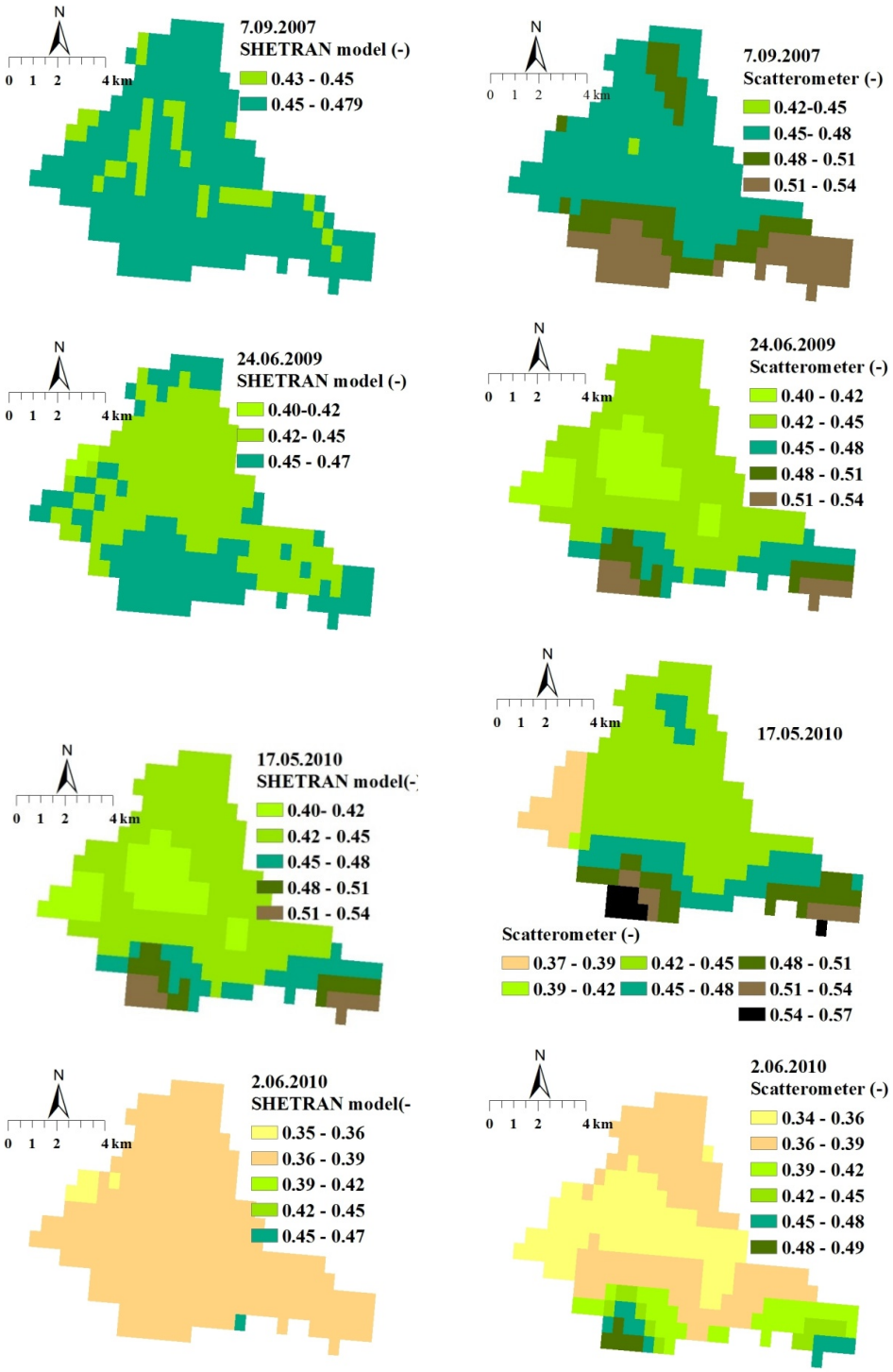

Fig. 5. The spatial patterns of the maximum surface soil moisture simulated by the SHETRAN hydrologic model (left) and estimated by downscaling from the scatterometer (right) for the days of the peak runoff occurring: 7 September 2007; 24 June 2009; 17 May 2010 and 2 June 2010.

Table 5. The assessment of the agreement between the two spatially distributed soil moisture estimates for the Jičinka River catchment according to criterion functions: CR3, CR4, MAE, R, RMSE and d (average/ minimum /maximum values).

Criterion	Calibration rain event	Validation rain events		
	September 2007	June 2009	May 2010	June 2010
CR3	–0.28/–4.35/0.30	–0.495/–1.387/0	–1.45/–5.1/–0.02	–2.5/–7/–0.34
CR4	0.89/0.62/0.99	0.81/0.71/0.999	0.76/0.56/0.99	0.72/0.58/0.999
MAE	0.07/0.04/0.30.0	0.09/0.05/0.37	0.11/0.05/0.16	0.11/0.04/0.25
R	0.8/0.06/0.995	0.63/0.004/0.99	0.68/0.12/0.99	0.71/0.196/0.99
RMSE	0.096/0.08/0.196	0.11/0.06/0.15	0.12/0.05/0.18	0.13/0.05/0.17
d	0.55/0.18/0.66	0.51/0.15/0.91	0.49/0.24/0.68	0.41/0.15/0.53

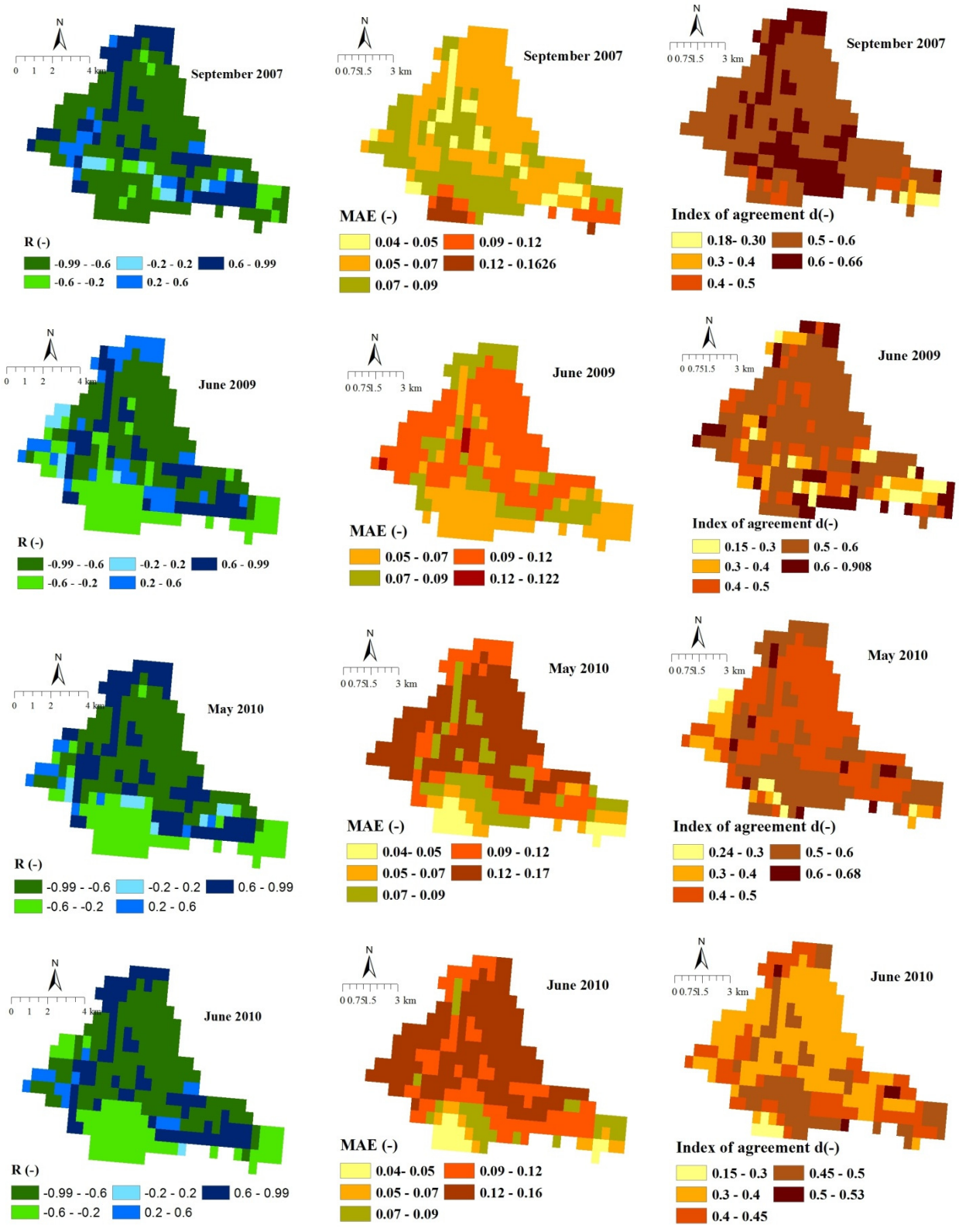

Fig. 6. The spatial distribution of the correlation coefficient, the mean absolute error and the index of agreement across the Jičinka River catchment for the analyzed rain events in September 2007, June 2009, May 2010 and June 2010.

The consistency between the two sources of soil moisture information was spatially analyzed in terms of the same evaluation criteria which were used for the evaluation of the hydrological model performance. The spatial distribution of the correlation coefficient, the mean absolute error and the index of agreement are shown in Fig. 6. The determined average, minimum and maximum values of the applied evaluation criteria at the level of the Jičinka River catchment are also shown in Table 5.

It should be noted that negative values of criteria CR1 – CR3 were obtained when soil moisture estimates from the two different sources were compared. The values of criteria CR3, which ranges from –7 to 0.3, are shown in Table 5. However,

the obtained negative values do not indicate the lack of agreement between the two types of soil moisture estimates. This result was obtained because spatial and temporal differences in soil moisture are small in very wet conditions which prevail during the analyzed intensive rain events. Although the differences between the soil moisture values from the hydrological model and derived from satellite data are not significant, in cases of all the analyzed rain events, the temporal differences between the satellite derived soil moisture values for a grid cell and its average value are smaller. In that way, negative values of the evaluation criteria CR1 to CR3 were reached. On the other hand, the better values of the other evaluation criteria (Table 5 and Fig. 6) signify that there is a correlation between the two types of soil moisture estimates. The average values of the coefficient of correlation at the catchment level are in the range between 0.625 to the 0.797, while the average values of the index of agreement are in the range between 0.413 to 0.717. The obtained results are satisfactory if we take into account that there is a considerable amount of uncertainty in soil moisture estimated by both the hydrological model and by downscaling from microwave remote sensing.

A comparison between the simulated soil moisture of large-scale hydrological models and satellite derived soil moisture was performed for many areas across the world (Alvarez-Gorreton et al., 2016; Badou et al., 2018; Brocca et al., 2011; Laiolo et al et al., 2014; Lopez et al., 2017; Parajka et al., 2009; Wanders et al.,2013; Xiong et al., 2018). Good agreement was often obtained between these two sources of soil moisture estimation. On the basis of the results obtained in these studies, it was concluded that the use of remotely sensed soil moisture data in calibration and parameter identification of large-scale hydrological models contributed to a better simulation of soil moisture content over the catchment and better discharge simulations.

This study has shown that downscaled soil moisture data may also be used as additional criteria for the calibration and validation of distributed hydrological models in small catchments, since good correlation was obtained between the two types of soil moisture estimates in this study. This type of analysis was not performed in previous studies. In that way, the use of satellite derived soil moisture data can reduce parameter uncertainty and improve rainfall-runoff modeling and the accuracy of flood predictions for small catchments. Similarly to the previously obtained results for large basins, it can be concluded that downscaled remote sensed soil moisture can be potentially used to improve the understanding of hydrological processes in small cathments.

5 CONCLUSION

Accurate soil moisture information is very important for flood forecasting. Due to variation in climate, soil, vegetation, topography and other factors, soil moisture content is highly variable in time and space. The knowledge of spatio-temporal dynamics of soil moisture within the catchment can improve the estimation of runoff and contribute to a better understanding of hydrological processes in catchments.

In this study the comparison of spatial and temporal dynamics of soil moisture, estimated from the physically based and distributed SHETRAN hydrological model and by downscaling from satellite soil moisture data was performed on the example of the small Jičinka River catchment (75.9 km^2) in the Czech Republic. The SHETRAN model was calibrated and verified on the basis of observed streamflow hydrographs at the catchment outlet.

On the basis of the results of the evaluation criteria it can be concluded that a good correlation between spatially and temporally distributed soil moisture values estimated from the SHETRAN model and by downscaling from the satellite soil moisture data was obtained. The results of the evaluation criteria indicate that soil moisture values obtained by downscaling satellite data can be used as additional criteria for the calibration and validation of hydrological models in small catchments. In that way, downscaled satellite soil moisture data can facilitate and improve model parameterization and runoff simulations by reducing uncertainties in calibration and validation of hydrological models for small catchments. Although both sources of soil moisture information have certain limitations and uncertainties, their integrated use could improve hydrological simulations.

Acknowledgements. This paper is a result of scientific collaboration between the Department of Ecological Engineering for Soil and Water Resources Protection at the Faculty of Forestry, University of Belgrade and the Institute of Landscape Water Management at the Faculty of Civil Engineering, Brno University of Technology. This paper was supported by the Czech National Agency for Agricultural Research (Project No. QK1720303), the Technology Agency of the Czech Republic (Project No. TH04030363) and by the Ministry of Education, Science and Technological Development, Republic of Serbia (Grant No. TR43007).

REFERENCES

Albergel, C., Calvet, J.C., Mahfouf, J.F., Rüdiger, C., Barbu, A.L., Lafont, S., Roujean, J.L., Walker, J.P., Crapeau, M., Wigneron, J.P., 2010. Monitoring of water and carbon fluxes using a land data assimilation system: A case study for southwestern France. Hydrology and Earth System Sciences, 14, 1109–1124. DOI: 10.5194/hess-14-1109-2010

Alvarez-Garreton, C., Ryu, D., Western, A.W., Crow, W.T., Su, C.-H., Robertson, D.R., 2016. Dual assimilation of satellite soil moisture to improve streamflow prediction in data-scarce catchments. Water Resour. Res., 52, 5357–5375. DOI: 10.1002/2015WR018429

Badou, D.F., Diekkruger, B., Montzka, C., 2018. Validation of satellite soil moisture in the absence of in situ soil moisture: the ecase of the Tropical Yankin Basin. South African Journal of Geomatics, 7, 3. http://dx.doi.org/10.4314/sajg.v7i3.3

Beven, K., 2006. A manifesto for the equifinality thesis. Journal of Hydrology, 320, 18–30.

Brocca, L., Melone, F., Moramarco, T., Wagner, W., Naeimi, V., Bartalis, Z., Hasenauer, S., 2010. Improving runoff prediction through the assimilation of the ASCAT soil moisture product. Hydrology and Earth System Sciences, 14, 1881–1893. DOI:10.5194/hess-14-1881-2010

Brocca, L., Hasenauer, S., Lacava, T., Melone, F., Moramarco, T., Wagner, W., Dorigo, W., Matgen, P., Martinez-Fernandez, J., Llorens, P., et al., 2011. Soil moisture estimation through ascat and amsr-e sensors: An intercomparison and validation study across europe. Remote Sens. Environ., 115, 3390–3408.

Chiew, F., McMahon, T., 1994. Application of the daily rainfall–runoff model MODHYDROLOG to 28 Australian catchments. Journal of Hydrology, 153, 383–416.

Corradini, C., 2014. Soil moisture in the development of hydrological processes and its determination at different spatial scales. J. Hydrol., 516, 1–5.

Crow, W.T., Berg, A.A., Cosh, M.H., Loew, A., Mohanty,

B.P., Panciera, R., de Rosnay, P., Ryu, D., Walker, J.P., 2012. Upscaling sparse ground-based soil moisture observations for the validation of coarse-resolution satellite soil moisture products. Rev. Geophys., 50, 2. https://doi.org/10.1029/2011RG000372

Dai, Y., Xin, Q.,Wei, N., Zhang, Y., Shangguan,W.,Zuan, H., Zhang, Z., Liu,S., Lu, X., 2019. A global high-resolution data set of soil hydraulic and thermal properties for land surface modelling. Journal of Advances in Modelling Earth Systems, 11, 9, 2996–3023. https://doi.org/10.1029/2019MS001784

Danhelka, J., Kubat J., Šercl P., Čekal, R. (Eds.), 2014. Floods in the Czech Republic in June 2013. Czech Hydrometeorological Institute, Prague, Czech Republic.

Dorigo, W.A., Wagner, W., Albergel, C., Albrecht, F., Balsamo, G., Brocca, L., Chung, D., Ertl, M., Forkel, M., Gruber, A., Haas, E., Hamer, D.P., Hirschi, M., Ikonen, J., De Jeu, R., Kidd, R., Lahoz, W., Liu, Y.Y., Miralles, D., Lecomte, P., 2017. ESA CCI Soil Moisture for improved Earth system understanding: State-of-the art and future directions. Remote Sensing of Environment, 203, 185–215. https://doi.org/10.1016/j.rse.2017.07.001

Đukić, V., Radić, Z., 2014. GIS based estimation of sediment discharge and areas of soil erosion and deposition for the torrential Lukovska River Catchment in Serbia. Water Resources Management, 28, 13, 4567–4581. https://link.springer.com/article/10.1007/s11269-014-0751-7

Đukić, V., Radić, Z., 2016. Sensitivity analysis of a physically based distributed model. Water Resources Management, 3, 1669–1684. https://link.springer.com/article/10.1007/s11269-016-1243-8

Ewen, J., Parkin, G., O'Connell, P.E., 2000. SHETRAN: Distributed river basin flow and transport modelling system. ASCE J. Hydrologic Eng., 5, 250–258. Available at: https://research.ncl.ac.uk/shetran/SHETRAN_ASCE_paper.pdf

Gruber, A., Dorigo, W.A., Crow, W., Wagner, W., 2017. Triple collocation-based merging of satellite soil moisture retrievals. IEEE Transactions on Geoscience and Remote Sensing, 55, 12, 1–13. https://doi.org/10.1109/TGRS.2017.2734070

Gruber, A., Scanlon, T., van der Schalie, R., Wagner, W., Dorigo, W., 2019. Evolution of the ESA CCI Soil Moisture Climate Data Records and their underlying merging methodology. Earth System Science Data, 11, 717–739. https://doi.org/10.5194/essd-11-717-2019

Gwak, Y., Kim, S., 2017. Factors affecting soil moisture spatial variability for a humid forest hillslope. Hydrol. Processes, 31, 431–445.

Hengl, T., Mendes de Jesus, J., Heuvelink, G.B.M., Ruiperez Gonzalez, M., Kilibarda, M., Blagoti´c, A., Shangguan, W., Wright, M.N., Geng, X., Bauer-Marschallinger, B., et al., 2017. Soilgrids 250 m: Global gridded soil information based on machine learning. PLoS ONE, 12, e0169748.

Hupet, F., Vanclooster, M., 2002. Intraseasonal dynamics of soil moisture variability within a small agricultural maize cropped field. J. Hydrol., 261, 86–101.

IPCC, 2012. Managing the risks of extreme events and disasters to advance climate change adaptation. A Special Report of Working Groups I and II of the Intergovernmental Panel on Climate Change [Field, C.B., V. Barros, T.F., Stocker, D., Qin, D.J., Dokken, K.L., Ebi, M.D., Mastrandrea, K.J., Mach, G.-K., Plattner, S.K., Allen, M.T., Midgley, P.M. (eds.)]. Cambridge University Press, Cambridge, UK, and New York, NY, USA, 582 p.

Jackson, T.J., Cosh, M.H., Bindlish, R., Starks, P.J., Bosch, D.D., Seyfried, M., Goodrich, D.C., Moran, M.S., Du, J., 2010. Validation of advanced microwave scanning radiometer soil moisture products. IEEE Transactions on Geoscience and Remote Sensing, 48, 12, 4256–4272. DOI: 10.1109/TGRS.2010.2051035

Koster, R.D., Mahanama, S.P.P., Livneh, B., Lettenmaier, D.P., Reichle, R.H., 2010. Skill in streamflow forecasts derived from large - scale estimates of soil moisture and snow. Nature Geosciences, 3, 613–616. DOI: 10.1038/ngeo944

Koster, R.D., Brocca, L., Crow, W.T., Burgin, M.S., De Lannoy, G.J.M., 2016. Precipitation estimation using l-band and c-band soil moisture retrievals. Water Resour. Res., 52, 7213–7225.

Laiolo, P., Gabellani, S., Pulvirenti, L., Boni, G., Rudari, R., et. al., 2014. Validation of remote sensing soil moisture products with a distributed continuous hydrological model. In: IEEE Geoscience and Remote Sensing Symposium. Quebec City, pp. 3319–3322. DOI: 10.1109/IGARSS.2014.6947190.

Lievens, H., S.K., Tomer, A., Al Bitar, G., De Lannoy, M., Drusch, G., Dumedah, H.-J. H., Franssen, Y., Kerr, B., Martens, Pan, M., 2015. SMOS soil moisture assimilation for improved hydrologic simulation in the Murray Darling Basin, Australia. Remote Sens. Environ., 168, 146–162.

López López, P., Sutanudjaja, E.H., Schellekens, J., Sterk, G., and Bierkens, M.F.P., 2017. Calibration of a large-scale hydrological model using satellite-based soil moisture and evapotranspiration products. Hydrol. Earth Syst. Sci., 21, 3125–3144. https://doi.org/10.5194/hess-21-3125-2017.

Manfreda, S., McCabe, M.F., Fiorentino, M., Rodriguez-Iturbe, I., Wood, E.F., 2007. Scaling characteristics of spatial patterns of soil moisture from distributed modelling. Adv. Water Resour., 30, 2145–2150.

Molnar, D.K., Julien, P.Y., 2000. Grid-size effects on surface runoff modelling. Journal of Hydrologic Engineering, 5, 1.

Montzka, C., Rötzer, K., Bogena, H.R., Sanchez, N., Vereecken, H., 2018. A new soil moisture downscaling approach for SMAP, SMOS, and ASCAT by predicting sub-grid variability. Remote Sens., 10, 427.

Mualem, Y., 1976. A new model predicting the hydraulic conductivitynof unsaturated porous media. Water Resour. Res., 12, 513–522.

Nash, J.E., Sutcliffe, J.V., 1970. River flow forecasting through conceptual models: Part I. A discussion of principles. Journal of Hydrology, 27, 3, 282–290.

Pavlik, F., Dumbrovský, M., 2014. Influence of landscape retention capacity upon flood processes in Jičínka River basin. Acta Universitatis Agriculturae et Silviculturae Mendelianae Brunensis, 62, 1, 191–199. DOI: 10.11118/actaun201462010191

Parajka, J., Naeimi, V., Blöschl, G., Wagner, W., Merz, R., Scipal, K., 2006. Assimilating scatterometer soil moisture data into conceptual hydrologic models at the regional scale. Hydrol. Earth Syst. Sci., 10, 353–368.

Parajka, J., Naeimi, V., Blöschl, G., Komma, J., 2009. Matching ERS scatterometer based soil moisture patterns with simulations of a conceptual dual layer hydrologic model over Austria. Hydrol. Earth Syst. Sci., 13, 259–271, https://doi.org/10.5194/hess-13-259-2009

Peng, J., Loew, A., Zhang, S., Wang, J., Niesel, J., 2017. Spatial downscaling of satellite soil moisture data using a Vegetation Temperature Condition Index. IEEE Trans. Geosci. Remote Sens., 54, 1, 558–566.

Pereira, A.R., Pruitt, W.O., 2004. Adaptation of the Thornthwaite scheme for estimating daily reference evapotranspiration. Agricultural Water Management, 66, 3, 251–257.

Qu, W., Bogena, H.R., Huisman, J.A., Vanderborght, J., Schuh, M., Priesack, E., Vereecken, H., 2015. Predicting subgrid variability of soil water content from basic soil information. Geophys. Res. Lett., 42, 789–796.

Richards, L.A., 1931. Capillary conduction of liquids through porous mediums. Physics, 1, 5, 318–333. DOI: 10.1063/1.1745010

Rodell, M., Houser, P., Jambor, U., Gottschalck, J., Mitchell, K., Meng, C.-J., Arsenault, K., Cosgrove, B., Radakovich, J., Bosilovich, M., 2004. The global land data assimilation system. Bull. Am. Meteorol. Soc., 85, 381–394. https://doi.org/10.1175/BAMS-85-3-381

Rosenbaum, U., Bogena, H.R., Herbst, M., Huisman, J.A., Peterson, T.J., Weuthen, A., Western, A.W., Vereecken, H., 2012. Seasonal and event dynamics of spatial soil moisture patterns at the small catchment scale. Water Resour. Res., 48, 10. https://doi.org/10.1029/2011WR011518

Rötzer, K., Montzka, C., Bogena, H., Wagner, W., Kerr, Y.H., Kidd, R., Vereecken, H., 2014. Catchment scale validation of smos and ascat soil moisture products using hydrological modeling and temporal stability analysis. J. Hydrol., 519, 934–946.

Saint-Venant, A.J.C.B., 1871. Théorie du mouvement non permanent des eaux, avec application aux crues des rivières et a l'introduction de marées dans leurs lits. Comptes rendus hebdomadaires des séances de l'Académie des sciences, 73, 147–154, 237–240.

Stoorvogel, J.J., Bakkenes, M., Temme, A.J.A.M., Batjes, N.H., ten Brink, B.J.E., 2017. S-world: A global soil map for environmental modelling. Land Degrad. Dev., 28, 22–33.

Shangguan, W., Dai, Y.J., Duan, Q.Y., Liu, B.Y., Yuan, H., 2014. A global soil data set for earth system modeling. J. Adv. Model. Earth Syst., 6, 249–263.

Srivastava, P.K., Han, D., Rico-Ramirez, M.A., Islam, T., 2013. Appraisal of SMOS soil moisture at a catchment scale in a temperate maritime climate. Journal of Hydrology, 498, 292–304.

Teuling, A.J., Troch, P.A., 2005. Improved understanding of soil moisture variability dynamics. Geophys. Res. Lett., 32.

Thiessen, A.H., 1911. Precipitation averages for large areas. Monthly Weather Review, 39, 7, 1082–1084. http://dx.doi.org/10.1175/1520-0493(1911)39<1082b: PAFLA>2.0.CO;2

van Genuchten, M.T., 1980. A closed-form equation for predicting the hydraulic conductivity of unsaturated soils. Soil Sci. Soc. Am. J., 44, 892–898.

Vereecken, H., Huisman, J.A., Pachepsky, Y., Montzka, C., van der Kruk, J., Bogena, H., Weihermüller, L., Herbst, M., Martinez, G., Vanderborght, J., 2014. On the spatio-temporal dynamics of soil moisture at the field scale. J. Hydrol., 516, 76–96.

Verhoest, N.E.C., et al., 2015. Copula-based downscaling of coarse-scale soil moisture observations with implicit bias correction, IEEE Trans.Geosci. Remote Sens., 53, 6, 3507–3521.

Wanders, N., Bierkens, M.F.P., Jong, S.M., Roo, A., Karssenberg, D., 2013. The benefits of using remotely sensed soil moisture in parameter identification of large-scale hydrological models. Water Resour. Res., 50, 6874–6891. DOI: 10.1002/2013WR014639

Wang, L., Qu, J.J., 2009. Satellite remote sensing applications for surface soil moisture monitoring: a review. Frontiers of Earth Science in China, 3, 2, 237–247.

Western, A.W., Grayson, R.B., Bloschl, G., Willgoose, G.R., McMahon, T.A., 1999. Observed spatial organization of soil moisture and its relation to terrain indices. Water Resour. Res., 35, 797–810.

Xiong, L., Yang, H., Zeng, L., Xu, C.-Y., 2018. Evaluating Consistency between the Remotely Sensed Soil Moisture and the Hydrological Model-Simulated Soil Moisture in the Qujiang Catchment of China. Water, 10, 3, 291. https://doi.org/10.3390/w10030291

Ye, W., Bates, B.C., Viney, N.R., Silvapan, M., Jakeman, A.J., 1997. Performance of conceptual rainfall–runoff models in low-yielding ephemeral catchments. Water Resources Research, 33, 1, 153–166.

Received 27 September 2019
Accepted 23 September 2020